Adaptive Deep Neural Network-Based Control Barrier Functions

Hannah M. Sweatland, Omkar Sudhir Patil, and Warren E. Dixon

Abstract—Safety constraints of nonlinear control systems are commonly enforced through the use of control barrier functions (CBFs). Uncertainties in the dynamic model can disrupt forward invariance guarantees or cause the state to be restricted to an overly conservative subset of the safe set. In this paper, adaptive deep neural networks (DNNs) are combined with CBFs to produce a family of controllers that ensure safety while learning the system's dynamics in real-time without the requirement for pre-training. By basing the least squares adaptation law on a state derivative estimator-based identification error, the DNN parameter estimation error is shown to be uniformly ultimately bounded. The convergent bound on the parameter estimation error is then used to formulate CBF-constraints in an optimization-based controller to guarantee safety despite model uncertainty. Furthermore, the developed method is extended for use under intermittent loss of state-feedback. A switched systems analysis for CBFs is provided with a maximum dwell-time condition during which the feedback can be unavailable. Comparative simulation results demonstrate the ability of the developed method to ensure safety in an adaptive cruise control problem and when feedback is lost, unlike baseline methods. Results show improved performance compared to baseline methods and demonstrate the ability of the developed method to ensure safety in feedback-denied environments.

I. Introduction

Control barrier functions (CBFs) enforce state constraints necessary for safe operation of control systems [1], [2], but CBF-based control input constraints depend on the dynamic model of the system. As a result, uncertainties in modeling the dynamics can endanger safety. To address challenges posed by the modeling uncertainty, robust safety methods can be used, where safety guarantees are provided using the worst-case bounds on the uncertainty. However, robust methods yield an overly conservative constraint on the control input that restricts the state to a subset of the safe set.

Adaptive CBFs have been developed to ensure the forward invariance of a safe set through online parameter adaptation [3]–[6]. Because the adaptive CBFs in both [3] and [4] include the parameter estimation error, the state is restricted to a subset of the safe set, dependent on the upper-bound of the estimation error. Methods such as set membership identification [4], integral concurrent learning [7], and parameter-adaptive CBFs [6] reduce the conservativeness with sufficient data, but these methods involve a white-box approach where the uncertainty

is required to have a known structure based on traditional modeling techniques. In contrast, recent results such as [8]–[10] use black-box models such as pre-trained deep neural networks (DNNs) and Gaussian processes to identify uncertain dynamics using training datasets and therefore reduce conservativeness; however, since these methods are not adaptive, they result in static models that may become obsolete over time. Moreover, the offline methods often require large datasets that may not be available prior to execution in completely unknown environments.

Other recent works reduce conservativeness of the CBF-based constraints by combining CBFs with disturbance observers [10]–[13]. Disturbance observers are used to produce an estimate of the uncertainty which is then used in the CBF constraint, expanding the state's operating region when compared to a robust approach. Adaptive safety is achieved in [10] through a modular approach that can combine a pre-trained DNN model with a robust integral sign of the error (RISE)-based disturbance observer, eliminating conservativeness of the safe set over time. Although disturbance observers can estimate general nonlinear and time-varying uncertainties, the estimates are only instantaneous and do not involve a model that can be used for subsequent predictions. In contrast, models such as DNNs can extrapolate through unexplored regions and can be employed to ensure safety under intermittent loss of feedback. Therefore, instead of using disturbance observers or pre-trained DNNs as in [10]–[13] it is desirable to construct adaptive CBFs using DNNs such as those in [14]–[18] with analytic real-time adaptation laws without the need for pre-training. Previous Lyapunov-based (Lb-) DNN adaptive controllers address the trajectory tracking problem; however, the tracking error-based adaptation laws in such results are not suitable for the adaptive safety problem since safety does not typically require tracking error convergence. Thus, in the developed work, a novel weight adaptation law is formulated to instead yield function approximation error convergence.

In this paper, adaptive DNN CBFs (aDCBFs) are developed to ensure safety while learning the system's uncertain dynamics in real-time. This paper provides the first result combining CBFs with an adaptive DNN that updates in real-time, eliminating the need for pre-training. The DNN adaptation law is not based on the tracking error as in all previous Lb-DNN literature. Instead, a least squares adaptation law is designed by constructing an identification error. Since computing an identification error requires state-derivative information, an interlaced approach is used where a secondary state-derivative estimator is combined with the adaptive DNN to generate the adaptation laws. A combined Lyapunov-based analysis yields guarantees on the DNN function approximation. The

convergent upper-bound of the parameter estimation error is then used to formulate candidate CBF-based constraints in an optimization-based control law to guarantee the forward invariance of the safe set, while reducing the conservative behavior often seen in robust approaches. As a result, during intermittent loss of feedback, the DNN can be used to make open-loop predictions that are used to reformulate CBF-based constraints to guarantee safety. Thus, the developed method can be used for safe operation of uncertain systems in environments with feedback occlusion zones, where intermittent loss of feedback typically occurs. A switched systems analysis for CBFs is provided with a maximum dwell-time condition during which the feedback can be unavailable. Comparative simulation results are presented to demonstrate the performance of the developed method on two control systems with baseline results in [1] and [10].

II. NOTATION AND PRELIMINARIES

Let $\mathbb{R}_{\geq 0} \triangleq [0, \infty)$, $\mathbb{R}_{>0} \triangleq (0, \infty)$, and $\mathbb{R}^{n \times m}$ represent the space of $n \times m$ dimensional matrices. The identity matrix of size n is denoted by I_n. The p-norm is denoted by $\|\cdot\|_p$, $\|\cdot\|$ is the 2-norm, and $\|\cdot\|_F$ is the Frobenius norm defined as $\|\cdot\|_F \triangleq \|\text{vec}(\cdot)\|$, where $\text{vec}(\cdot)$ denotes the vectorization operator. Given some matrix $A \triangleq [a_{i,j}] \in \mathbb{R}^{n \times m}$, where $a_{i,j}$ denotes the element in the ith row and j^{th} column of A, the vectorization operator is defined as $\text{vec}(A) \triangleq [a_{1,1}, \ldots, a_{n,1}, \ldots, a_{1,m}, \ldots, a_{n,m}]^\top \in \mathbb{R}^{nm}$. Let the notation $[d]$ be defined as $[d] \triangleq \{1, 2, \ldots, d\}$ and, for vectors $x \in \mathbb{R}^n$ and $y \in \mathbb{R}^m$, let $(x, y) \triangleq [x^\top, y^\top]^\top$. For a set $B \subset \mathbb{R}^n$, the boundary of B is denoted ∂B, the interior of B is denoted $\text{int}(B)$, and an open neighborhood about B is denoted $\mathcal{N}(B)$. A set-valued mapping $M : B \rightrightarrows \mathbb{R}^m$ associates every point $x \in B$ with a set $M(x) \subset \mathbb{R}^m$.

A. Deep Neural Network Model

For simplicity in the illustration, a fully-connected DNN will be described here. The following control and adaptation law development can be generalized for any network architecture Φ with a corresponding Jacobian Φ'. The reader is referred to [19] and [20] for extending the subsequent development to ResNets and LSTMs, respectively. Let $\sigma \in \mathbb{R}^{L_{\text{in}}}$ denote the DNN input with size $L_{\text{in}} \in \mathbb{Z}_{>0}$, and $\theta \in \mathbb{R}^p$ denote the vector of DNN parameters (i.e., weights and bias terms) with size $p \in \mathbb{Z}_{>0}$. A fully-connected feedforward DNN $\Phi(\sigma, \theta)$ with output size $L_{\text{out}} \in \mathbb{Z}_{>0}$ is defined using a recursive relation $\Phi_j \in \mathbb{R}^{L_{j+1}}$ given by [14]

$$\Phi_j \triangleq \begin{cases} V_j^\top \phi_j(\Phi_{j-1}), & j \in [k], \\ V_j^\top \sigma_a, & j = 0, \end{cases} \qquad (1)$$

where $\Phi(\sigma, \theta) = \Phi_k$, and $\sigma_a \triangleq [\sigma^\top \ 1]^\top$ denotes the augmented input that accounts for the bias terms, $k \in \mathbb{Z}_{>0}$ denotes the total number of hidden layers, $V_j \in \mathbb{R}^{L_j \times L_{j+1}}$ denotes the matrix of weights and biases, and $L_j \in \mathbb{Z}_{>0}$ denotes the number of nodes in the jth layer for all $j \in \{0, \ldots, k\}$ with $L_0 \triangleq L_{\text{in}} + 1$ and $L_{k+1} = L_{\text{out}}$. The vector of smooth activation functions is denoted by $\phi_j :$

$\mathbb{R}^{L_j} \rightarrow \mathbb{R}^{L_j}$ for all $j \in [k]$. If the DNN involves multiple types of activation functions at each layer, then ϕ_j may be represented as $\phi_j \triangleq [\varsigma_{j,1} \ \ldots \ \varsigma_{j,L_j-1} \ 1]^\top$, where $\varsigma_{j,i} : \mathbb{R} \rightarrow \mathbb{R}$ denotes the activation function at the ith node of the jth layer. For the DNN architecture in (1), the vector of DNN weights is $\theta \triangleq [\text{vec}(V_0)^\top \ \ldots \ \text{vec}(V_k)^\top]^\top$ with size $p = \Sigma_{j=0}^k L_j L_{j+1}$. The Jacobian of the activation function vector at the jth layer is denoted by $\phi_j' : \mathbb{R}^{L_j} \rightarrow \mathbb{R}^{L_j \times L_j}$, and $\phi_j'(y) \triangleq \frac{\partial}{\partial z} \phi_j(z)\big|_{z=y}, \ \forall y \in \mathbb{R}^{L_j}$. Let the Jacobian of the DNN with respect to the weights be denoted by $\Phi'(\sigma, \theta) \triangleq \frac{\partial}{\partial \theta} \Phi(\sigma, \theta)$, which can be represented using $\Phi'(\sigma, \theta) = [\Phi_0', \ \Phi_1', \ \ldots, \ \Phi_k']$, where $\Phi_j' \triangleq \frac{\partial}{\partial \text{vec}(V_j)} \Phi(\sigma, \theta)$ for all $j \in [k]$. Then, using (1) and the property $\frac{\partial}{\partial \text{vec}(B)} \text{vec}(ABC) = C^\top \otimes A$ [21, Proposition 7.1.9] yields $\Phi_0' = \left(\overset{\curvearrowleft}{\prod_{l=1}^k} V_l^\top \phi_l'(\Phi_{l-1}) \right) (I_{L_1} \otimes \sigma_a^\top)$ and

$$\Phi_j' = \left(\overset{\curvearrowleft}{\prod_{l=j+1}^k} V_l^\top \phi_l'(\Phi_{l-1}) \right) (I_{L_{j+1}} \otimes \phi_j^\top(\Phi_{j-1})), \text{ for all}$$

$j \in [k]$, where the notation $\overset{\curvearrowleft}{\prod}$ denotes the right-to-left matrix product operation, i.e., $\overset{\curvearrowleft}{\prod_{p=1}^m} A_p = A_m \ldots A_2 A_1$ and $\overset{\curvearrowleft}{\prod_{p=a}^m} A_p = I$ if $a > m$, and $\otimes$ denotes the Kronecker product.

III. PROBLEM FORMULATION

A. Dynamic Model

Consider the nonlinear dynamic system

$$\dot{x} = f(x) + g(x)u, \qquad (2)$$

where $x \in \mathbb{R}^n$ denotes the state, $f : \mathbb{R}^n \rightarrow \mathbb{R}^n$ denotes an unknown continuously differentiable function, $u \in \Psi \subset \mathbb{R}^m$ denotes the control input, and $g : \mathbb{R}^n \rightarrow \mathbb{R}^{n \times m}$ denotes the known control effectiveness matrix, where $\Psi : \mathbb{R}^n \rightrightarrows \mathbb{R}^m$ denotes the set of admissible control inputs. The control objective is to design a controller that ensures the forward invariance of a safe set $\mathcal{S} \subset \mathbb{R}^n$ despite uncertainty in $f(x)$. Forward invariance is a common safety objective because trajectories beginning inside a forward invariant safe set will remain in the safe set.

Given a controller $\kappa : \mathbb{R}^n \rightarrow \mathbb{R}^m$ with $\kappa(x) \in \Psi(x)$ for all $x \in \mathbb{R}^n$, we refer to the closed-loop dynamics defined by (2) and κ as $f_{cl}(x) \triangleq f(x) + g(x)\kappa(x)$. A solution to the closed-loop dynamics $t \mapsto x(t)$ is complete if $\text{dom}x$ is unbounded and maximal if there is no solution y such that $x(t) = y(t)$ for all $t \in \text{dom}x$, where $\text{dom}x$ is a proper subset of $\text{dom}y$. The set $\mathcal{S}$ is forward pre-invariant for the closed-loop dynamics $\dot{x} = f_{cl}(x)$ if, for each $x_0 \in \mathcal{S}$ and each maximal solution x starting from x_0, $x(t) \in \mathcal{S}$ for all $t \in \text{dom}x$ [22, Definition 2.5]. The set is forward invariant for the closed-loop dynamics if it is forward pre-invariant and additionally, for each $x_0 \in \mathcal{S}$, every maximal solution x starting from x_0 is complete [22, Definition 2.6].

B. Control Barrier Functions (CBFs)

CBFs are a method used to encode a system's safety requirements. Using the development in [23], multiple scalar-valued CBF candidates can be used to define the safe set.

Definition 1. [23, Def. 1] A vector-valued function $B : \mathbb{R}^n \rightarrow \mathbb{R}^d$ is a CBF candidate defining a safe set $\mathcal{S} \subset \mathbb{R}^n$ if $\mathcal{S} = \{x \in \mathbb{R}^n : B(x) \leq 0\}$, where $B(x) \triangleq (B_1(x), B_2(x), \ldots, B_d(x))$. Also let $\mathcal{S}_i \triangleq \{x \in \mathbb{R}^n : B_i(x) \leq 0\}$ and $M_i \triangleq \{x \in \partial\mathcal{S} : B_i(x) = 0\}$ for each $i \in [d]$.

The state constraints defined by the CBF candidate can then be translated to constraints on the control input, through the introduction of a performance function $\gamma : \mathbb{R}^n \rightarrow \mathbb{R}^d$. The design parameter γ limits the worst-case growth of B to ensure forward invariance of $\mathcal{S}$ based on conditions derived in [24].

Definition 2. A continuously differentiable CBF candidate $B : \mathbb{R}^n \rightarrow \mathbb{R}^d$ defining the set $\mathcal{S} \subset \mathbb{R}^n$ is a CBF for (2) and $\mathcal{S}$ on a set $\mathcal{O} \subset \mathbb{R}^n$ with respect to a function $\gamma : \mathbb{R}^n \rightarrow \mathbb{R}^d$ if 1) there exists a neighborhood of the boundary of $\mathcal{S}$ such that $\mathcal{N}(\partial\mathcal{S}) \subset \mathcal{O}$, 2) the function γ is such that, for each $i \in [d]$, $\gamma_i(x) \geq 0$ for all $x \in \mathcal{N}(M_i)\backslash\mathcal{S}_i$, and 3) the set

$$K_c(x) \triangleq \left\{ u \in \Psi(x) : \nabla B^\top(x)(f(x) + g(x)u) \leq -\gamma(x) \right\} \tag{3}$$

is nonempty for every $x \in \mathcal{O}$.

Since $f(x)$ is unknown, the inequality defining K_c in (3) cannot be guaranteed to be satisfied without using a conservative bound on the dynamics that would restrict the state's operating region to a subset of the safe set. Thus, there is motivation to develop an estimate of the uncertain dynamics to expand the operating region. DNNs are a powerful tool that can be used to produce a real-time approximation of $f(x)$.

C. Deep Neural Network (DNN) Approximation

Based on the universal function approximation theorem, DNNs can be used to approximate continuous functions that lie on a compact set [25]. Lyapunov-based methods have been developed to update the layer weights of a number of neural network (NN) architectures including fully-connected DNNs [14], long short-term memory NNs [20], deep recurrent NNs [18], and deep residual NNs (ResNets) [19].

On a compact set $\Omega \subset \mathbb{R}^n$, the uncertain dynamics in (2) can be modeled as

$$f(x) = \Phi(x, \theta^*) + \varepsilon(x), \tag{4}$$

where $\Phi : \mathbb{R}^n \times \mathbb{R}^p \rightarrow \mathbb{R}^n$ denotes the selected DNN architecture, $\theta^* \in \mathbb{R}^p$ denotes a vector of ideal weights defined as $\theta^* \triangleq \arg\min_\theta \sup_{x \in \Omega} \left(\|f(x) - \Phi(x, \theta)\|^2 + \sigma \|\theta\|^2 \right)$, where $\sigma \in \mathbb{R}_{>0}$ is a regularizing constant, and $\varepsilon : \mathbb{R}^n \rightarrow \mathbb{R}^n$ denotes the unknown function reconstruction error. By the universal function approximation property, for any prescribed $\overline{\varepsilon} \in \mathbb{R}_{>0}$, there exist ideal DNN weights such that $\sup_{x \in \Omega} \|f(x) - \Phi(x, \theta^*)\| \leq \overline{\varepsilon}$. The function approximation error in (4) satisfies $\sup_{x \in \Omega} \|\varepsilon(x)\| \leq \overline{\varepsilon}$ on the compact domain

Ω. The subsequent CBF analysis ensures the input to the DNN, x, remains in the forward invariant safe set $\mathcal{S} \subseteq \Omega$ for all time, so the universal function approximation property can be applied.

The DNN has a nested nonlinearly parameterized structure, so traditional adaptive control techniques used for linearly parameterized systems are not applicable. To help overcome the complexities introduced by the nonlinearities, a first-order Taylor series approximation can be used to estimate $\Phi(x, \theta^*)$ as [14]

$$\Phi(x, \theta^*) = \Phi\left(x, \hat{\theta}\right) + \Phi'\tilde{\theta} + \Delta_O^2\left(\left\|\tilde{\theta}\right\|\right), \tag{5}$$

where $\hat{\theta} \in \mathbb{R}^p$ denotes a vector composed of the adaptive estimates of the DNN layer weights that are generated using the subsequently designed adaptation laws, $\Phi' \in \mathbb{R}^{n \times p}$ denotes the Jacobian of the DNN architecture defined as $\Phi' \triangleq \frac{\partial \Phi(x, \hat{\theta})}{\partial \hat{\theta}}$, $\tilde{\theta} \in \mathbb{R}^p$ denotes the weight estimation error defined as $\tilde{\theta} \triangleq \theta^* - \hat{\theta}$, and $\Delta_O^2 : \mathbb{R}^p \rightarrow \mathbb{R}^n$ denotes higher-order terms. The following assumption is made to facilitate the subsequent analysis.

Assumption 1. There exists a known constant $\overline{\theta} \in \mathbb{R}_{>0}$ such that the unknown ideal weights can be bounded as $\|\theta^*\| \leq \overline{\theta}$ [26, Assumption 1]. Additionally, there exists a known constant $\Xi \in \mathbb{R}_{>0}$ such that $\|f(x) - \Phi(x, \theta)\|^2 + \sigma \|\theta\|^2$ is strictly convex with respect to θ for all $\theta \in \mathcal{B} \triangleq \{\vartheta \in \mathbb{R}^p : \|\theta^* - \vartheta\| \leq \Xi\}$.

Remark 1. In Assumption 1, local convexity of the regularized loss function $\|f(x) - \Phi(x, \theta)\|^2 + \sigma \|\theta\|^2$ is assumed to facilitate convergence to a local minimum in the subsequent analysis. A number of theoretical results in deep learning literature that indicate that for some DNN architectures such as deep ResNets, every local minimum is a global minimum [27]–[30]. Furthermore, the regularizing term $\sigma \|\theta\|^2$ assists in convexifying the loss function and mitigating practical issues in deep learning such as overfitting [31, Chapter 7]. The strict convexity assumption on the loss function ensures that θ^* is unique.

Substituting the DNN estimate in (4) and Taylor series approximation in (5) into the left-hand side of the inequality in (3) yields

$$\dot{B}(x, u) = \nabla B^\top(x)\left(\Phi\left(x, \hat{\theta}\right) + \Phi'\tilde{\theta} + \Delta + g(x)u\right), \tag{6}$$

where $\Delta \in \mathbb{R}^n$ is defined as $\Delta \triangleq \Delta_O^2\left(\left\|\tilde{\theta}\right\|\right) + \varepsilon(x)$. Although the DNN approximation alone is less conservative than bounding the entire uncertainty, (6) is still composed of the unknown terms $\tilde{\theta}$ and Δ. Assumption 1 could be used to bound $\tilde{\theta}$ in the CBF constraint in (6), but instead we introduce an adaptive identifier in the following subsection to further reduce conservative behavior due to the uncertainty in $\tilde{\theta}$.

D. Adaptive DNN-Based Identifier Design

All previous Lb-DNN-based adaptive control results update the DNN weights using the tracking error [14], [17]–[20], [32]; however, the objective in those results is to track a desired

trajectory. To achieve adaptive safety, the adaptive weight updates need to be performed with system identification as the objective. Therefore, a least squares weight adaptation law is introduced to adaptively identify the system dynamics based on an identification error. Performing least squares-based real-time identification is challenging for continuous-time systems because it requires state-derivative information which is often unknown or noisy. Therefore, we introduce a high-gain state-derivative estimator defined as

$$\dot{\hat{x}} = \hat{f} + g\left(x\right)u + k_x\tilde{x}, \tag{7}$$

$$\dot{\hat{f}} = k_f\left(\dot{\tilde{x}} + k_x\tilde{x}\right) + \tilde{x}, \tag{8}$$

where $\hat{x}, \hat{f} \in \mathbb{R}^n$ denote the observer estimates of x and f, respectively, $k_x, k_f \in \mathbb{R}_{>0}$ are positive constant observer gains, and observer errors $\tilde{x}, \tilde{f} \in \mathbb{R}^n$ are defined as $\tilde{x} \triangleq x - \hat{x}$ and $\tilde{f} \triangleq f\left(x\right) - \hat{f}$, respectively. Since state feedback is available, $\tilde{x}$ is known, but $\dot{\tilde{x}}$ is unknown. An implementable form of $\hat{f}$ can be found by integrating both sides of $\dot{\hat{f}}$ in (8) to yield $\hat{f}\left(t\right) = \hat{f}\left(t_0\right) + k_f\tilde{x}\left(t\right) - k_f\tilde{x}\left(t_0\right) + \int_{t_0}^{t}\left(k_f k_x + 1\right)\tilde{x}\left(\tau\right)d\tau.$ Taking the time derivative of the definitions of $\tilde{x}$ and $\tilde{f}$ and substituting (7) and (8) yields

$$\dot{\tilde{x}} = \tilde{f} - k_x\tilde{x}, \tag{9}$$

$$\dot{\tilde{f}} = \dot{f} - k_f\tilde{f} - \tilde{x}, \tag{10}$$

where $\dot{f}\left(x\right) \triangleq \nabla f^\top\left(x\right)\dot{x}$. The following lemma is provided to establish the boundedness of $\dot{f}$ based on the continuous differentiability of f under common assumptions in CBF literature.

Lemma 1. *Consider the function f, a continuous controller $\kappa \in \Psi$ and the set $\mathcal{S} \subset \mathbb{R}^n$. Based on the continuous differentiability of f, the continuity κ, and the boundedness of x on $\mathcal{S}$, the signals f and κ are bounded on $\mathcal{S}$. Therefore, there exists a known constant $\bar{\dot{f}} \in \mathbb{R}_{>0}$ such that $\left\|\dot{f}\left(x\right)\right\| \leq \bar{\dot{f}}$ for all $x \in \mathcal{S}$.*

Proof: The safe set $\mathcal{S}$ is compact because it is a closed subset of the compact set Ω. Because of the continuity of f and the fact that $\mathcal{S}$ is compact, there exists a known constant $\bar{f} \in \mathbb{R}_{\geq 0}$ such that $\|f\left(x\right)\| \leq \bar{f}$ for all $x \in \mathcal{S}$. The controller κ and control effectiveness g are continuous and therefore bounded for all $x \in \mathcal{S}$. Thus, because $\dot{x} = f\left(x\right) + g\left(x\right)\kappa\left(x\right)$, it follows that $\dot{x}$ is bounded for all $x \in \mathcal{S}$ based on the boundedness of f, x, and κ on $\mathcal{S}$. The function f is continuously differentiable, so ∇f is bounded on $\mathcal{S}$. Since $\dot{f}\left(x\right) = \nabla f^\top\left(x\right)\dot{x}$, there exists a constant $\bar{\dot{f}} \in \mathbb{R}_{>0}$ such that $\left\|\dot{f}\left(x\left(t\right)\right)\right\| \leq \bar{\dot{f}}$ for all $x \in \mathcal{S}$. ∎

Figure 1 provides a visualization of the sets Ω and $\mathcal{S}$. The CBF constraints restrict the state trajectories to the safe set $\mathcal{S}$, where $\left\|\dot{f}\left(x\right)\right\| \leq \bar{\dot{f}}$. Because $\mathcal{S} \subseteq \Omega$, the universal function approximation property of DNNs holds on $\mathcal{S}$.
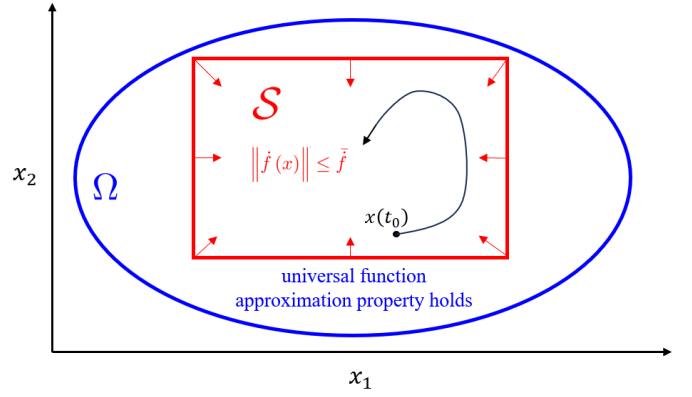

Figure 1. An illustration of the sets Ω and $\mathcal{S}$ in $\mathbb{R}^2$. On the blue set Ω the universal function approximation property holds. Flows generated by the CBF are constrained to the red set $\mathcal{S}$, where $\left\|\dot{f}\left(x\right)\right\| \leq \bar{\dot{f}}$.

Based on the subsequent analysis, the DNN adaptation law $\dot{\hat{\theta}} \in \mathbb{R}^p$ is designed as

$$\dot{\hat{\theta}} = \text{proj}\left(\Gamma\left(-k_\theta\hat{\theta} + \alpha\Phi'^\top\left(x, \hat{\theta}\right)\left(\hat{f} - \Phi\left(x, \hat{\theta}\right)\right)\right)\right), \tag{11}$$

where $k_\theta, \alpha \in \mathbb{R}_{>0}$ denote constant gains and the projection operator $\text{proj}\left(\cdot\right)$ is defined as in [33, Appendix E] and ensures that $\hat{\theta}\left(t\right) \in \mathcal{B}$. The term $\Gamma \in \mathbb{R}^{p \times p}$ denotes a symmetric positive-definite time-varying least squares adaptation gain matrix that is a solution to

$$\frac{d}{dt}\Gamma^{-1} = -\beta\left(t\right)\Gamma^{-1} + \Phi'^\top\left(x, \hat{\theta}\right)\Phi'\left(x, \hat{\theta}\right), \tag{12}$$

with the bounded-gain time-varying forgetting factor $\beta : \mathbb{R}_{\geq 0} \to \mathbb{R}_{\geq 0}$ designed as $\beta\left(t\right) \triangleq \beta_0\left(1 - \frac{\|\Gamma\|}{\kappa_0}\right)$, where $\beta_0, \kappa_0 \in \mathbb{R}_{>0}$ are user-defined constants that denote the maximum forgetting rate and the bound prescribed on $\|\Gamma\|$, respectively. The adaptation gain matrix is initialized to be positive-definite such that $\|\Gamma\left(t_0\right)\| < \kappa_0$, and $\Gamma\left(t\right)$ remains positive-definite for all $t \in \mathbb{R}_{\geq 0}$ [34]. Because $\Gamma\left(t\right)$ is positive-definite, there exists a constant $\kappa_1 \in \mathbb{R}_{>0}$ such that $\lambda_{\min}\left(\Gamma\left(t\right)\right) \geq \kappa_1$ for all $t \in \mathbb{R}_{\geq t_0}$. If $\Phi'\left(x, \hat{\theta}\right)$ satisfies the persistence of excitation (PE) condition, meaning there exist constants $\varphi_1, \varphi_2 \in \mathbb{R}_{>0}$ such that $\varphi_1 I_p \leq \int_{t_1}^{t_1+T}\Phi'^\top\left(x\left(\tau\right), \hat{\theta}\left(\tau\right)\right)\Phi'\left(x\left(\tau\right), \hat{\theta}\left(\tau\right)\right)d\tau \leq \varphi_2 I_p$ for all $t_1 \in \mathbb{R}_{\geq 0}$ and $T \in \mathbb{R}_{>0}$, it can be shown that $\beta_1 > 0$ [34, Sec. 4.2], where $\beta_1 \in \mathbb{R}_{\geq 0}$ is a constant such that $\beta \geq \beta_1$.

IV. STABILITY ANALYSIS

Taking the time derivative of $\tilde{\theta}$, adding and subtracting f, and substituting (4) and (5) into (11), the parameter estimation error dynamics are given as

$$\dot{\tilde{\theta}} = -\text{proj}\left(\Gamma\left(k_\theta\hat{\theta} + \alpha\Phi'^\top\left(x, \hat{\theta}\right)\left(\Phi'\tilde{\theta} + \Delta - \tilde{f}\right) - k_\theta\theta^*\right)\right). \tag{13}$$

The subsequent Lyapunov-based stability analysis demonstrates the convergence properties of (9), (10), and (13).

To facilitate the stability analysis, let $z \triangleq \begin{bmatrix} \tilde{x}^\top & \tilde{f}^\top & \tilde{\theta}^\top \end{bmatrix}^\top \in \mathbb{R}^{2n+p}$ denote the concatenated state vector. Let the Lyapunov function candidate $V : \mathbb{R}^{2n+p} \to \mathbb{R}$ be defined as

$$V(z) \triangleq \frac{1}{2}\tilde{x}^\top \tilde{x} + \frac{1}{2}\tilde{f}^\top \tilde{f} + \frac{1}{2}\tilde{\theta}^\top \Gamma^{-1}\tilde{\theta}, \qquad (14)$$

which can be bounded as

$$\lambda_1 \|z\|^2 \leq V(z) \leq \lambda_2 \|z\|^2, \qquad (15)$$

where $\lambda_1 \triangleq \min\left\{\frac{1}{2}, \frac{1}{2\kappa_0}\right\}$, $\lambda_2 \triangleq \max\left\{\frac{1}{2}, \frac{1}{2\kappa_1}\right\}$. Taking the time-derivative of (14), substituting (9), (10), (12), and (13), and applying the property of projection operators $-\tilde{\theta}^\top \Gamma^{-1}\text{proj}(\mu) \leq -\tilde{\theta}^\top \Gamma^{-1}\mu$ [33, Lemma E.1.IV], yields

$$\dot{V} \leq -k_x \|\tilde{x}\|^2 - k_f \left\|\tilde{f}\right\|^2 + \tilde{f}^\top \dot{f}$$
$$- \left(\frac{\beta_1}{2\kappa_0} + k_\theta\right)\left\|\tilde{\theta}\right\|^2 - \left(\alpha - \frac{1}{2}\right)\tilde{\theta}^\top \Phi'^\top\left(x, \hat{\theta}\right)\Phi'\left(x, \hat{\theta}\right)\tilde{\theta}$$
$$+ \alpha\tilde{\theta}^\top \Phi'^\top\left(x, \hat{\theta}\right)\left(\tilde{f} - \Delta\right) + k_\theta\tilde{\theta}^\top \theta^*. \qquad (16)$$

Because f and Φ are continuously differentiable $\|\Delta\| \leq c_1$ and $\left\|\Phi'\left(x, \hat{\theta}\right)\right\|_F \leq c_2$ when $z \in \mathcal{D} \triangleq \left\{\zeta \in \mathbb{R}^{2n+p} : \|\zeta\| \leq \chi\right\}$, where $c_1, c_2, \chi \in \mathbb{R}_{>0}$ are known constants. Recall that by Lemma 1, there exists a known bound $\overline{\dot{f}} \in \mathbb{R}_{>0}$ such that $\left\|\dot{f}\right\| \leq \overline{\dot{f}}$ for all $x \in \mathcal{S}$. Using Young's Inequality and Assumption 1, $\tilde{\theta}^\top \Phi'^\top\left(x, \hat{\theta}\right)\left(\tilde{f} - \Delta\right) \leq c_2 \left\|\tilde{\theta}\right\|^2 + \frac{c_2}{2}\left\|\tilde{f}\right\|^2 + \frac{c_2 c_1^2}{2}$, $\tilde{f}^\top \dot{f} \leq \frac{\overline{\dot{f}}}{2}\left\|\tilde{f}\right\|^2 + \frac{\overline{\dot{f}}}{2}$, and $k_\theta\tilde{\theta}^\top \theta^* \leq \frac{k_\theta}{2}\left\|\tilde{\theta}\right\|^2 + \frac{k_\theta}{2}\overline{\theta}^2$, so (16) can be further bounded as

$$\dot{V} \leq -\lambda_3 \|z\|^2 + C - \left(\alpha - \frac{1}{2}\right)\tilde{\theta}^\top \Phi'^\top\left(x, \hat{\theta}\right)\Phi'\left(x, \hat{\theta}\right)\tilde{\theta}, \qquad (17)$$

where $\lambda_3 \triangleq \min\left\{k_x, \ k_f - \frac{\overline{\dot{f}}}{2} - \frac{c_2}{2}, \ \frac{\beta_1}{2\kappa_0} + \frac{k_\theta}{2} - c_2\right\}$ and $C \triangleq \frac{\overline{\dot{f}} + c_2 c_1^2 + k_\theta\overline{\theta}^2}{2}$. Additionally, let $\mathcal{Q} \triangleq \left\{\zeta \in \mathbb{R}^{2n+p} : \|\zeta\| \leq \sqrt{\frac{\lambda_1}{\lambda_2}\chi^2 - \frac{C}{\lambda_3}}\right\}$, which is defined to initialize z in the subsequent analysis. The following theorem provides conditions under which the adaptation law in (11) yields parameter estimation error convergence.

Theorem 1. *Let $t \mapsto x(t)$ be such that $x(t_0) \in int(\mathcal{S})$[1] and there exists a time interval $\mathcal{I} \triangleq [t_0, t_\mathcal{I})$ such that $x(t) \in \mathcal{S}$ for all $t \in \mathcal{I}$. If Assumption 1 is satisfied, κ is continuous, and $\chi > \sqrt{\frac{\lambda_2 C}{\lambda_1\lambda_3}}$, then the weight update law in (11) ensures that $\left\|\tilde{\theta}(t)\right\| \leq \tilde{\theta}_{UB}(t)$ for all $t \in \mathcal{I}$, where*

$$\tilde{\theta}_{UB}(t) \triangleq \sqrt{\frac{\lambda_2}{\lambda_1}\|z(t_0)\|^2 e^{-\frac{\lambda_3}{\lambda_2}t} + \frac{\lambda_2 C}{\lambda_1\lambda_3}\left(1 - e^{-\frac{\lambda_3}{\lambda_2}t}\right)},$$

provided $z(t_0) \in \mathcal{Q}$, $\hat{\theta}(t_0) \in \mathcal{B}$, $\lambda_3 > 0$, and $\alpha > \frac{1}{2}$.

Proof: From the Lyapunov function candidate in (14) and the inequalities in (15) and (17), $\dot{V}$ can be further bounded as

[1]The initial conditions $x(t_0)$ is considered to be in the interior of $\mathcal{S}$ to ensure $\mathcal{I}$ is not measure-zero, thus ruling out solutions that instantly escape $\mathcal{S}$.

$\dot{V} \leq -\frac{\lambda_3}{\lambda_2}V + C$, for all $z \in \mathcal{D}$ and $t \in \mathcal{I}$ if the gain conditions are satisfied. Solving the differential inequality over the time interval $\mathcal{I}$ yields

$$V(z(t)) \leq V(z(t_0))e^{-\frac{\lambda_3}{\lambda_2}t} + \frac{\lambda_2 C}{\lambda_3}\left(1 - e^{-\frac{\lambda_3}{\lambda_2}t}\right), \quad (18)$$

for all $z \in \mathcal{D}$. From (14) and (18), it follows that

$$\|z(t)\| \leq \sqrt{\frac{\lambda_2}{\lambda_1}\|z(t_0)\|^2 e^{-\frac{\lambda_3}{\lambda_2}t} + \frac{\lambda_2 C}{\lambda_1\lambda_3}\left(1 - e^{-\frac{\lambda_3}{\lambda_2}t}\right)}, \quad (19)$$

for all $z \in \mathcal{D}$ and $t \in \mathcal{I}$. To ensure $z(t) \in \mathcal{D}$ for all $t \in \mathcal{I}$, further upper-bounding (19) yields $\|z(t)\| \leq \sqrt{\frac{\lambda_2}{\lambda_1}\|z(t_0)\|^2 + \frac{\lambda_2 C}{\lambda_1\lambda_3}}$ for all $t \in \mathcal{I}$; hence, $z(t) \in \mathcal{D}$ always holds if $\sqrt{\frac{\lambda_2}{\lambda_1}\|z(t_0)\|^2 + \frac{\lambda_2 C}{\lambda_1\lambda_3}} \leq \chi$, which is guaranteed if $\|z(t_0)\| \leq \sqrt{\frac{\lambda_1}{\lambda_2}\chi^2 - \frac{C}{\lambda_3}}$, i.e., $z(t_0) \in \mathcal{Q}$. Thus, trajectories of z do not escape $\mathcal{D}$ if z is initialized in $\mathcal{Q}$. Additionally, because $\left\|\tilde{\theta}\right\| \leq \|z\|$, (19) implies

$$\left\|\tilde{\theta}(t)\right\| \leq \sqrt{\frac{\lambda_2}{\lambda_1}\|z(t_0)\|^2 e^{-\frac{\lambda_3}{\lambda_2}t} + \frac{\lambda_2 C}{\lambda_1\lambda_3}\left(1 - e^{-\frac{\lambda_3}{\lambda_2}t}\right)}, \quad (20)$$

for all $t \in \mathcal{I}$ and $z \in \mathcal{D}$ if $z(t_0) \in \mathcal{Q}$. For the initial conditions to be feasible, $\mathcal{Q}$ is required to be non-empty, which is ensured by selecting $\chi > \sqrt{\frac{\lambda_2 C}{\lambda_1\lambda_3}}$. $\blacksquare$

The bound in (20) cannot be implemented without information about the concatenated initial state $z(t_0)$. Since the state information is available, $\hat{x}$ is initialized such that $\tilde{x}(t_0) = 0$. While $\tilde{f}$ and $\tilde{\theta}$ are unknown, each have known bounds. Recall that because of the continuity of f and the fact that $\mathcal{S}$ is a closed subset of the compact set Ω and is therefore compact, there exists a known constant $\overline{f} \in \mathbb{R}_{\geq 0}$ such that $\|f(x)\| \leq \overline{f}$ for all $x \in \mathcal{S}$. Thus, it follows that $\tilde{f}$ is bounded. The bound on $\tilde{\theta}$ is a result of the projection operator in (13). If $\left\|\hat{f}(t_0)\right\| \leq \overline{f}$ and $\hat{\theta}(t_0) \in \mathcal{B}$, then $\left\|\tilde{f}(t_0)\right\| \leq 2\overline{f}$ and $\left\|\tilde{\theta}(t_0)\right\| \leq \Xi$. Therefore, there exists a known constant $\mathcal{Z} \in \mathbb{R}_{>0}$ such that $\|z(t_0)\| \leq \mathcal{Z} \triangleq \sqrt{\Xi^2 + 4\overline{f}^2}$ and (20) can be further bounded as

$$\left\|\tilde{\theta}(t)\right\| \leq \sqrt{\frac{\lambda_2}{\lambda_1}\mathcal{Z}^2 e^{-\frac{\lambda_3}{\lambda_2}t} + \frac{\lambda_2 C}{\lambda_1\lambda_3}\left(1 - e^{-\frac{\lambda_3}{\lambda_2}t}\right)}, \quad (21)$$

for all $t \in \mathcal{I}$ if $z(t_0) \in \mathcal{Q}$.

Because the bound in (21) may initially be more conservative than Ξ, we design a function $\chi_\theta \in \mathbb{R}_{>0}$ as

$$\chi_\theta \triangleq \min\left\{\Xi, \sqrt{\frac{\lambda_2}{\lambda_1}\mathcal{Z}^2 e^{-\frac{\lambda_3}{\lambda_2}t} + \frac{\lambda_2 C}{\lambda_1\lambda_3}\left(1 - e^{-\frac{\lambda_3}{\lambda_2}t}\right)}\right\}, \quad (22)$$

such that $\left\|\tilde{\theta}(t)\right\| \leq \chi_\theta$ for all time. When the observer gains k_x and k_f are selected to be sufficiently high, $\lambda_3 = \frac{\beta_1}{2\kappa_0} + \frac{k_\theta}{2} - c_2$, which implies the rate of convergence in (21) depends primarily on β_1 and k_θ. Thus, when the PE condition is satisfied, $\beta_1 > 0$, resulting in a larger λ_3 which implies χ_θ converges faster and to a smaller value. When the PE condition is not satisfied, the gain k_θ helps achieve the uniform ultimate boundedness of $\tilde{\theta}$ based on sigma modification; however, selection of a larger k_θ yields a larger C, worsening parameter

estimation performance. By substituting the developed upper-bound of the parameter estimation error in (22) into (6) and recalling $\|\Delta\| \leq c_1$, a new CBF notion composed of only the known signals can be defined.

Definition 3. A continuously differentiable CBF candidate $B : \mathbb{R}^n \to \mathbb{R}^d$ defining the set $\mathcal{S} \subseteq \Omega$ is an *adaptive DNN CBF (aDCBF)* for the dynamics in (2) and safe set $\mathcal{S}$ on a set $\mathcal{O} \subset \mathbb{R}^n$ with respect to $\gamma : \mathbb{R}^n \to \mathbb{R}^d$ if 1) there exists a neighborhood of the boundary of $\mathcal{S}$ such that $\mathcal{N}(\partial\mathcal{S}) \subset \mathcal{O}$, 2) for each $i \in [d]$, $\gamma_i(x) \geq 0$ for all $x \in \mathcal{N}(M_i) \backslash \mathcal{S}_i$, and 3) the set

$$K_d(x) \triangleq \left\{ u \in \Psi : \left\| \nabla B^\top(x) \Phi' \right\| (\chi_\theta + c_1) \right.$$
$$\left. + \nabla B^\top(x) \left(\Phi\left(x, \hat{\theta}\right) + g(x) u \right) \leq -\gamma(x) \right\},$$

is nonempty for all $x \in \mathcal{O}$.

The set K_d represents the set of control inputs that will render the set $\mathcal{S}$ forward invariant. A selection of K_d that minimizes some cost function can be made at each $x \in \mathcal{O}$ using an optimization-based control law.

The controller $\kappa^* : \mathbb{R}^n \to \Psi$ is defined as

$$\kappa^*(x) \triangleq \arg\min_{u \in \Psi} Q(x, u), \qquad (23)$$
$$\text{s.t. } \mathcal{C}_F(x, u) \leq 0,$$

where $Q(x, u) : \mathbb{R}^n \times \Psi \to \mathbb{R}$ is a cost function typically selected as $\|u - u_{nom}\|^2$, $u_{nom} \in \Psi$ is a nominal continuous control input, and $\mathcal{C}_F : \mathbb{R}^n \times \Psi \to \mathbb{R}^d$ are the constraints on the control input. By choosing $\mathcal{C}_F(x, u) \triangleq \left\| \nabla B^\top(x) \Phi' \right\| (\chi_\theta + c_1) + \nabla B^\top(x) \left(\Phi\left(x, \hat{\theta}\right) + g(x) u \right) + \gamma(x)$, the optimization problem yields a controller $\kappa^*(x) \in K_d$ for all $x \in \mathcal{O}$ assuming K_d is nonempty on the set $\mathcal{O}$. To obtain an implementable form of the controller, we impose the following conditions on the set of admissible control inputs Ψ.

Assumption 2. There exists a function $\psi : \mathbb{R}^n \times \mathbb{R}^m \to \mathbb{R}^s$ such that $\Psi(x) = \{u \in \mathbb{R}^m : \psi(x, u) \leq 0\}$ for all $x \in \mathbb{R}^n$. Additionally, for each $r \in [s]$, the function $u \mapsto \psi_r(x, u)$ is convex on K_d and $(x, u) \mapsto \psi(x, u)$ is continuous on $\mathcal{O} \times \mathbb{R}^m$.

The following lemma of [23, Theorem 4] provides conditions that result in a continuous κ^*.

Lemma 2. *[23, Theorem 4] Let $\mathcal{C} : \mathbb{R}^n \times \mathbb{R}^m \to \mathbb{R}^h$ be continuous on $\mathcal{O} \times \mathbb{R}^m$, and, for each $g \in [h]$, let $u \mapsto \mathcal{C}_g(x, u)$ be convex on the set $K(x) \triangleq \{u \in \mathbb{R}^m : \mathcal{C}_g(x, u) \leq 0, \forall g \in [h]\}$. Suppose $Q : \mathbb{R}^n \times \mathbb{R}^m \to \mathbb{R}$ is continuous and for each $x \in \mathcal{O}$, $u \mapsto Q(x, u)$ is strictly convex and inf-compact[2] on $K(x)$. If the set $K^\circ(x) \triangleq \{u \in \mathbb{R}^m : \mathcal{C}_g(x, u) < 0, \forall g \in [h]\}$ is nonempty for every $x \in \mathcal{O}$, then $\kappa^*(x) \triangleq \arg\min_{u \in K} Q(x, u)$ is continuous.*

The continuity of κ^* established in Lemma 2 allows Lemma 1 and Theorem 1 to be used in the proof of the following theorem, which presents the main result of this paper. The

implication of the theorem is that the developed DNN-based optimization problem in (23) ensures system trajectories beginning in the user-selected safe set $\mathcal{S}$ will remain in $\mathcal{S}$ for all time.

Theorem 2. *Suppose $B : \mathbb{R}^n \times \mathbb{R}^p \to \mathbb{R}$ is an aDCBF for the system defined by (2) and (23) defining a safe set $\mathcal{S} \subseteq \Omega$. Let $\hat{x}$, $\hat{f}$, and $\hat{\theta}$ update according to (7), (8), and (11), respectively. Let the system be initialized such that $\hat{x}(t_0) = x(t_0)$, $\left\|\hat{f}(t_0)\right\| \leq \overline{f}$, $z(t_0) \in \mathcal{Q}$, and $\hat{\theta}(t_0) \in \mathcal{B}$. If Assumptions 1 and 2 hold, Q is selected to be continuous, and $u \mapsto Q(x, u)$ is strictly convex and inf-compact on $K_d(x)$, then the safe set $\mathcal{S}$ is forward invariant for the closed-loop dynamics defined by (2), the controller κ^* in (23), and the adaptive weight update law in (11), provided $\lambda_3 > 0$.*

Proof: Let $t \mapsto x(t)$ be a solution to the closed-loop dynamics f_{cl} defined by (2) and (23). Because B is an aDCBF in the sense of Definition 3, the set $K_d(x)$ is nonempty on $\mathcal{O} \supset \mathcal{N}(\mathcal{S})$. Thus, the optimization-based control law in (23) yields a controller $\kappa^* \in K_d$. Because Q is continuous and $u \mapsto Q(x, u)$ is strictly convex and inf-compact on $K_d(x)$ by assumption, Assumption 2 holds, $\mathcal{C}_F$ is continuous on $\mathcal{O} \times \mathbb{R}^m$, and $u \mapsto \mathcal{C}_F(x, u)$ is convex on K_d. Therefore, the conditions of Lemma 2 hold, thus implying κ^* is single-valued and continuous on $\mathcal{O}$. By Lemma 1, there exists a constant $\bar{\bar{f}}$ such that $\left\|\dot{f}\right\| \leq \bar{\bar{f}}$ for all $x \in \mathcal{S}$, so Theorem 1 can be used to show that the weight update law in (11) ensures $\left\|\tilde{\theta}\right\|$ is uniformly ultimately bounded by (20) for all $t \in \mathcal{I}$. Since $\left\|\hat{f}(t_0)\right\| \leq \overline{f}$, $z(t_0) \in \mathcal{D}$, $\hat{\theta}(t_0) \in \mathcal{B}$, and f is continuously differentiable, it follows that $\left\|\tilde{\theta}(t_0)\right\| \leq \Xi$, $\left\|\tilde{f}(t_0)\right\| \leq 2\overline{f}$, and $\|\Delta\| \leq c_1$. Therefore, for every $u \in \Psi$ and $t \in \mathcal{I}$, $\nabla B^\top(x) \dot{x} \leq \left\| \nabla B^\top(x(t)) \Phi' \right\| (\chi_\theta + c_1) + \nabla B^\top(x(t)) \left(\Phi\left(x(t), \hat{\theta}\right) + g(x(t)) u \right)$, implying $\kappa^*(x(t)) \in K_d(x(t)) \subset K_c(x(t))$ for all $t \in \mathcal{I}$. Since K_d is nonempty for all $x \in \mathcal{O}$, K_c is nonempty on $\mathcal{O}$ and B is a CBF defining the set $\mathcal{S}$ in the sense of Definition 2. By Theorem 1 of [23], $\mathcal{S}$ is forward pre-invariant for the closed-loop dynamics defined by (2) and (23). Maximal solutions to f_{cl} are either complete or escape in finite-time by flowing [24, Proposition 3]. The safe set $\mathcal{S}$ is compact by definition, eliminating the possibility of finite-time escape from the safe set [35, Theorem 10.1.4], which implies all maximal solutions to the closed-loop system are complete, i.e., the maximal $\mathcal{I} = [t_0, \infty)$. Thus, it follows that the safe set $\mathcal{S}$ is forward invariant. ∎

V. Safety Under Intermittent State Feedback

During intermittent loss of feedback, the state measurements are not available, so it is impossible to use any feedback mechanisms; however, because the developed DNN yields parameter estimation error guarantees, it can be used to make state predictions at times when feedback is lost. Let $k \in \mathbb{Z}_{\geq 0}$ denote the time index such that feedback is unavailable in the time interval $[t_{2k+1}, t_{2k+2})$. When feedback is not available,

an open-loop estimation of the current state $\hat{X} \in \mathbb{R}^n$ can be updated according to

$$\dot{\hat{X}} = \Phi\left(\hat{X}, \hat{\theta}\left(t_{2k+1}\right)\right) + g\left(\hat{X}\right)u, \qquad (24)$$

where the initial condition for the state estimate is $\hat{X}\left(t_{2k+1}\right) = x\left(t_{2k+1}\right)$. When feedback becomes available, $\hat{X}(t)$ is reset as $\hat{X}(t) = x(t)$ for all $(t,k) \in [t_{2k}, t_{2k+1}) \times \mathbb{Z}_{\geq 0}$. In disturbance observer-based methods such as [10], the CBF-based constraint is reliant on the observer estimate of the dynamics and therefore on state measurements, so safety cannot be ensured when feedback is lost. In the developed approach, the constraint in (23) can be modified to ensure safety until feedback is restored.

A. Modified CBF Constraint Development

The open-loop estimator error $\tilde{X} \in \mathbb{R}^n$ is defined as $\tilde{X} \triangleq x - \hat{X}$; thus, $\tilde{X}\left(t_{2k+1}\right) = 0$. Exclusively for the purpose of this section, it is assumed that there exists a known constant $\bar{u} \in \mathbb{R}^n$ such that $\|u\| \leq \bar{u}$, for all $u \in \Psi$, the drift f is globally bounded and Lipschitz, and g is globally Lipschitz. Such an assumption on the boundedness of f is mild since finite-time escape is not inherent to the uncontrolled dynamics for most physical systems of practical interest. Based the assumptions on the boundedness of u and f and the continuous differentiability of Φ, there exists a Lipschitz constant $L_U \in \mathbb{R}_{>0}$ such that

$$\left\| \Phi\left(x, \theta^*\right) - \Phi\left(\hat{X}, \theta^*\right) + \left(g(x) - g\left(\hat{X}\right)\right)u \right\| \leq L_U \left\|\tilde{X}\right\|, \qquad (25)$$

and, additionally, there exists a constant $\Delta_U \in \mathbb{R}_{>0}$ such that

$$\left\| \Phi\left(\hat{X}, \theta^*\right) - \Phi\left(\hat{X}, \hat{\theta}\left(t_{2k+1}\right)\right) + \varepsilon(x) \right\| \leq \Delta_U. \qquad (26)$$

Let the Lyapunov function candidate during loss of feedback $V_U : \mathbb{R}^{2n+p} \to \mathbb{R}$ be defined as $V_U \triangleq \frac{1}{2} \tilde{X}^\top \tilde{X}$. Taking the time-derivative of V_U, adding and subtracting $\Phi\left(\hat{X}, \theta^*\right)$, substituting in (25) and (26), and using Young's Inequality, it can be shown that $\dot{V}_U \leq \lambda_U V_U + \frac{\Delta_U}{2}$ when feedback is unavailable, where $\lambda_U \triangleq 2L_U + \Delta_U$. Solving for V_U yields $V_U(t) \leq \left(V\left(t_{2k+1}\right) + \delta_U\right)e^{\lambda_U(t-t_{2k+1})} - \delta_U$ for all $(t,k) \in [t_{2k+1}, t_{2k+2}) \times \mathbb{Z}_{\geq 0}$, where $\delta_U \triangleq \frac{2\Delta_U}{2L_U + \Delta_U}$. Therefore, the open-loop estimation error dynamics can be shown to satisfy the form $\left\|\dot{\tilde{X}}\right\| \leq L_U \left\|\tilde{X}\right\| + \Delta_U$, which is exponentially unstable (cf., [36], [37]) such that

$$\left\|\tilde{X}(t)\right\| \leq \overline{\tilde{X}}(t) \triangleq \sqrt{\delta_U\left(e^{\lambda_U(t-t_{2k+1})} - 1\right)} \qquad (27)$$

for all $(t,k) \in [t_{2k+1}, t_{2k+2}) \times \mathbb{Z}_{\geq 0}$. The system dynamics can be bounded as $\|\dot{x}\| \leq \left\|\dot{\tilde{X}}\right\| + \left\|\dot{\hat{X}}\right\| \leq L_U \overline{\tilde{X}} + \Delta_U + \left\|\Phi\left(\hat{X}, \hat{\theta}\left(t_{2k+1}\right)\right) + g(x)u\right\|$, and if ∇B is locally Lipschitz, then $\left\|\nabla B^\top(x) - \nabla B^\top\left(\hat{X}\right)\right\| \leq \rho\tilde{X}(t)$, where $\rho \in \mathbb{R}_{>0}$ is a positive constant. Thus, the controller in (23) in absences of state feedback becomes

$$\kappa^*\left(\hat{X}\right) \triangleq \underset{u \in \Psi}{\arg\min} \, Q\left(\hat{X}, u\right),$$

$$\text{s.t. } \mathcal{C}_U\left(\hat{X}, u\right) \leq 0, \qquad (28)$$

where

$$\mathcal{C}_U\left(\hat{X}, u\right) \triangleq \overline{\tilde{X}}(t)\rho\left(L_U\overline{\tilde{X}}(t) + \Delta_U + \left\|\Phi\left(\hat{X}, \hat{\theta}\left(t_{2k+1}\right)\right)\right.\right.$$
$$\left. + g\left(\hat{X}\right)u\right\|\right) + \left\|\nabla B^\top\left(\hat{X}\right)\right\|\left(L_U\overline{\tilde{X}}(t) + \Delta_U\right)$$
$$+ \nabla B^\top\left(\hat{X}\right)\left(\Phi\left(\hat{X}, \hat{\theta}\left(t_{2k+1}\right)\right) + g\left(\hat{X}\right)u\right) + \gamma\left(\hat{X}\right). \qquad (29)$$

The development in Sections III and IV rely on the continuity of the control input u. When feedback is lost, the controller switches, introducing discontinuities. The constraint in (29) developed for intermittent loss of feedback is empirically tested in one of the following simulations. To account for the effects of switching, the following subsection introduces a switched systems analysis for CBFs with a dwell-time condition.

B. Maximum Loss of Feedback Dwell-Time Condition

As the time without feedback increases, the worst-case bound on $\tilde{X}$ grows exponentially, causing the constraint in (29) to shrink the system's operating region. To ensure the feasibility of the controller with the modified constraint in (29), a maximum loss of feedback dwell-time condition $\Delta t_k \in \mathbb{R}_{>0}$ can be developed using (27). In this subsection, it is additionally assumed that B is globally Lipschitz[3], implying that $\|\nabla B(x)\| \leq \bar{B}$, where $\bar{B} \in \mathbb{R}_{>0}$ is a known positive constant. To ensure the existence of a safety-ensuring control input, the time without feedback must be such that the inequality

$$\mathcal{C}_U\left(\hat{X}, u\right) - \mathcal{C}^*(x, u) \leq \bar{\mathcal{C}} \qquad (30)$$

is satisfied, where $\mathcal{C}^*(x, u) \triangleq \nabla B^\top(x)\dot{x}$ and $\bar{\mathcal{C}} \in \mathbb{R}^d$ is the user-selected maximum offset between the boundary of the safe set and the boundary of the operating region enforced by $\mathcal{C}_U$. Recall that, for the purpose of this section, the control input is assumed to be bounded such that $\|u\| \leq \bar{u}$, for all $u \in \Psi$. Substituting (29) into (30) and solving for $\Delta t_k \triangleq t_{2k+1} - t_{2k+2}$ yields a maximum loss of feedback dwell-time condition of

$$\Delta t_k \leq \frac{1}{\lambda_U}\ln\left(\frac{1}{\delta_U}\left(\left(\frac{\bar{\mathcal{C}} - 6\bar{B}\Delta_U - \mathcal{K}_U}{6L_U\bar{B}}\right)^2 + 1\right)\right), \qquad (31)$$

where $\mathcal{K}_U \triangleq 4\bar{B}\left\|\Phi\left(\hat{X}, \hat{\theta}\left(t_k\right)\right)\right\| + 4\bar{B}\left\|g\left(\hat{X}\right)\right\|\bar{u}$.

VI. SIMULATION STUDIES

Two simulations are provided to demonstrate the effectiveness of the developed aDCBFs. The optimization problem in (23) is used to define the control law with a cost function of $Q(x, u) = \|u - u_{nom}(x)\|^2$, where $u_{nom} \in \Psi$ is the nominal control input that tracks the desired trajectory.

A. Adaptive Cruise Control

In this section, the developed technique is applied to an adaptive cruise control (ACC) problem [1]. Suppose there are

---

[3]While a global Lipschitzness requirement may appear restrictive, many safe sets of practical interest such as polytopes (i.e., sets described by the intersection of hyperplanes) can be described using globally Lipschitz CBF candidates.
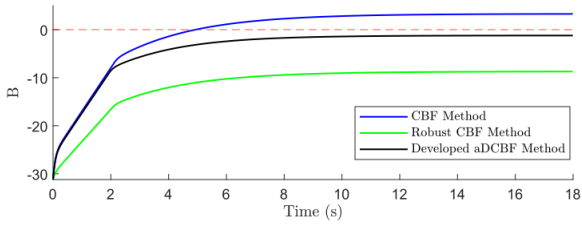
Figure 2. The value of the barrier functions over time for the ACC problem. A negative value of B indicates the follower vehicle remains in the safe set.

two vehicles traveling along a straight line. The lead vehicle travels forward with a velocity $v_{\text{lead}} \in \mathbb{R}$ of $v_{\text{lead}} = 10$ m/s, while the follower vehicle trails behind the lead vehicle. The follower vehicle has dynamics

$$\begin{bmatrix} \dot{x} \\ \dot{v} \end{bmatrix} = \begin{bmatrix} v \\ -\frac{1}{m}F_r(v) + \delta(v) \end{bmatrix} + \begin{bmatrix} 0 \\ \frac{1}{m} \end{bmatrix} u,$$

where $x \in \mathbb{R}$ is the position of the vehicle in meters, $v \in \mathbb{R}$ is the velocity of the vehicle in meters per second, $m \in \mathbb{R}$ is the mass in kg, the nonlinear function $F_r : \mathbb{R} \to \mathbb{R}$ represents the vehicle's rolling resistance, the function $\delta : \mathbb{R} \to \mathbb{R}$ represents an unknown disturbance, and $u \in \mathbb{R}$ is the control input. As described in [1], the rolling resistance is modeled as $F_r(v) = f_0 + f_1 v + f_2 v^2$, where $f_0 = 0.1$ N, $f_1 = 5 \frac{\text{N} \cdot \text{s}}{\text{m}}$, and $f_2 = 0.25 \frac{\text{N} \cdot \text{s}^2}{\text{m}}$. The added disturbance $\delta(v) = 30 \sin(0.1v)$ represents unmodeled forces on the vehicle and the mass of the vehicle is $m = 100$ kg. In the aDCBF method, the rolling resistance function is considered to be unknown and $f(x) = -\frac{1}{m}F_r(v) + \delta(v)$ is the nonlinear function that the DNN learns. The desired velocity of the follower vehicle $v_d \in \mathbb{R}$ is set to a constant $v_d \triangleq 20$ m/s. The distance between the lead and follower vehicles $D \in \mathbb{R}$ is defined as $D \triangleq x_{\text{lead}} - x$, where $x_{\text{lead}} \in \mathbb{R}$ is the position of the lead vehicle. The vehicles are initialized such that $v(t_0) = 16$ m/s, $v_{\text{lead}}(t_0) = 10$ m/s, and $D(t_0) = 60$ m. Because $v_{\text{lead}} < v_d$, the nominal velocity tracking controller defined as $u_{nom} \triangleq -\Phi\left(v, \hat{\theta}\right) - mk_1(v - v_d)$, where $k_1 = 10$ is a user-selected control gain, would eventually cause the follower vehicle to collide with the leader. The developed aDCBF approach is used to enforce a safe following distance. The safe set is defined as $\mathcal{S} \triangleq \{v \in \mathbb{R} : B(v) = -D + 1.8v \leq 0\}$, where 1.8 s represents the desired time headway as in [1]. A deep ResNet is used with 2 hidden layers, a shortcut connection between each layer, and 6 neurons in each layer, for a total of 122 individual layer weights. The weights are initialized from the normal distribution $N(0, 3)$ and the DNN gains are selected as $\Gamma(t_0) = 5I_{122}$, $k_\theta = 0.001$, $\beta_0 = 2$, and $\kappa_0 = 3$. The state-derivative estimator is used to produce the secondary estimate of f uses gains of $k_x = 5$ and $k_f = 10$. Figure 2 demonstrates how the controller in (23) with $\gamma(v) = 10B(v)$ is able to constrain the follower vehicle to a safe distance behind the lead vehicle.

Results for two comparison simulations are also provided in Figure 2. Using a standard CBF approach [1], the nominal controller is given access to F_r and m but does not have information about the disturbance term, meaning $u_{nom} \triangleq$

$F_r(v) - mk_1(v - v_d)$ and the CBF constraint is defined as $\mathcal{C}_F(v, u) \triangleq \dot{D} + 1.8\left(-\frac{1}{m}F_r(v) + \frac{1}{m}u\right) + 10B(v)$. The unmodeled uncertainty δ pushes the state trajectory out of the safe set (B reaches a positive steady-state value of 3.15, thus violating the safe following distance requirements). If it is known that the model of F_r is imperfect, a robust CBF approach can be used, with $u_{nom} \triangleq F_r(v) - m\bar{\delta} - mk(v - v_d)$ and $\mathcal{C}(v, u) \triangleq \dot{D} + 1.8\left(-\frac{1}{m}F_r(v) + \bar{\delta} + \frac{1}{m}u\right) + 10B(v)$, where $\bar{\delta} \in \mathbb{R}_{>0}$ is a known constant such that $\|\delta\| \leq \bar{\delta}$. Although the robust approach is able to keep the trajectory inside the safe set, the use of a worst-case bound on δ results in an overly conservative set of admissible controllers, restricting the state trajectory to a subset of the safe set. Using the robust CBF approach, B reaches a steady-state value of -8.81. Adaptive CBF methods such as those in [3] and [4] cannot be directly applied to this problem because of the nonlinearly parameterized uncertainty in δ. Using the developed method, B reaches a stead state value of -1.27. The developed aDCBF method ensures safety while reducing undesirable conservative behavior by 85.6%, compared to robust CBFs.

B. Non-Polynomial Dynamics

Consider the nonlinear dynamical system in (2) with $f(x) = \left[x_2 \sin(x_1) \tanh^2(x_2), \ x_1 x_2 \cos(x_2) \operatorname{sech}(x_2)\right]^\top$ and $g(x) = [1, 1]^\top$, where $x = [x_1, x_2]^\top$. White Gaussian noise was added to the position state measurement with a signal to noise ratio of 50 dB. The position state is initialized from the uniform distribution $U(-0.2, 0.2)$ with $\dot{x}(t_0) = [0, 0]^\top$, and the desired trajectory is defined as $x_d(t) = 0.1t[\sin(t), \ \cos(t)]^\top$. We define a vector-valued CBF as

$$B(x) \triangleq \begin{bmatrix} x_1 + x_2 - 2 \\ x_1 - x_2 - 2 \\ -x_1 + x_2 - 2 \\ -x_1 - x_2 - 2 \end{bmatrix},$$

which defines a diamond safe set $\mathcal{S} = \{x \in \mathbb{R}^2 : B(x) \leq 0\}$ with height and width of 4. The deep ResNet has 3 hidden layers, a shortcut connection across each hidden layer, and with 5 neurons in each layer, thus involving 174 total weights. The ResNet weights are initialized from the normal distribution $N(0, 0.5)$ and the DNN gains are selected as $\Gamma(t_0) = 5I_{174}$, $\alpha = 50$, $k_\theta = 0.001$, $\beta_0 = 2$, and $\kappa_0 = 10$. The state-derivative estimator is used to produce the secondary estimate of f using gains of $k_x = 10$ and $k_f = 5$. The nominal controller is defined as $u_{nom} = \dot{x}_d - \Phi\left(x, \hat{\theta}\right) - k_e(x - x_d)$, where $k_e = 10$. The function γ is selected as $\gamma(x) = 10B(x)$. Figure 3 shows the safe set and the desired and actual state trajectories. The simulation was run for 20 seconds with a step size of 0.005 seconds. To simulate performance under intermittent state feedback, the state measurement is made unavailable for 1 second intervals beginning at 10 seconds and 15 seconds, denoted by the orange $\times$ markers in Figure 3. During loss of feedback, the procedure in Section V is followed, where the identified DNN is used to make a prediction of the state and the modified robust CBF constraint in (29) is used to ensure safety. The method developed in Section V prevents the state
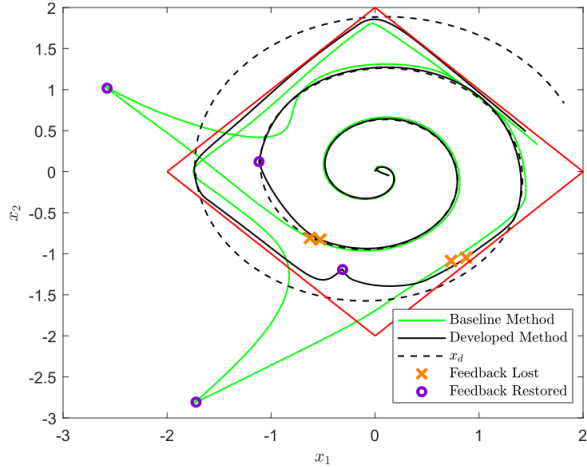
Figure 3. The state trajectory of the closed-loop system in Section VI-B using the developed aDCBF approach (black line) compared to the same control scheme without the ResNet approximation of the dynamics (green line).
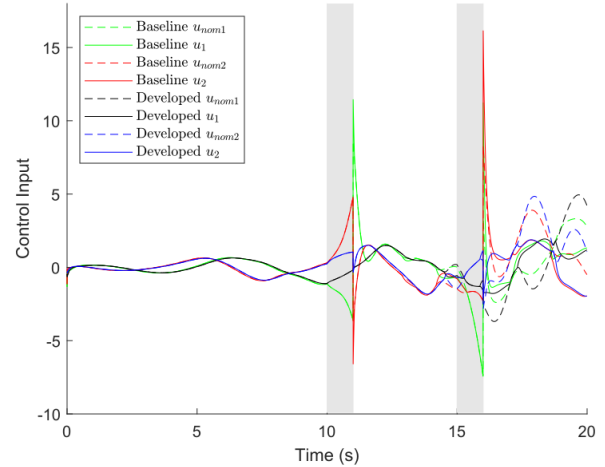

Figure 4. Comparison plots of the control inputs for the developed and baseline methods. The gray regions represent the time periods where state feedback is made unavailable.

from escaping the safe set until the feedback is restored at 11 seconds and 16 seconds, respectively, indicated by the purple ○ markers.

For the baseline method in [10], the nominal controller is $u_{nom} \triangleq \dot{x}_d - \hat{d} - k_e (x - x_d)$, where $\hat{d} \in \mathbb{R}^2$ represents the RISE-based disturbance observer estimate of f defined in [10, Eq. 6], and the CBF constraint in the optimization-based controller is $\mathcal{C}_F (x, u) \triangleq \left\| \nabla B^\top (x) \right\| \overline{f} + \nabla B^\top (x) g (x) u + \gamma (x)$. Though trajectory tracking performance is comparable to the developed approach at times when feedback is available, the state-derivative observer alone only provides an instantaneous estimate of the dynamics and fails to ensure safety in both instances of feedback loss, unlike the developed method. The nominal and implemented control inputs for the baseline and developed methods are shown in Figure 4. It can be seen that the developed controller in (23) with the selected cost function acts as a safety filter, modifying the nominal control input when the states get close to the boundary of the safe set and otherwise returning the same values as the nominal control input. Additionally, it can be seen that when feedback is made unavailable, the baseline controller reacts more aggressively causing spikes in the control input. The aggressive control action and violation of safety constraints are likely because the observer-based estimate of the dynamics is inaccurate under the loss of feedback. This inaccuracy is because, unlike the DNN model, the observer does not have the capacity to generalize beyond the explored trajectory points. However, because the developed method uses a DNN model that learns the dynamics online, the learned DNN is able to generalize on unseen trajectory points encountered during the loss of feedback. As a result, the optimization-based controllers in (23) and (28) ensure the safety constraints are satisfied while being less aggressive than the baseline controller.

Figure 5 shows the trajectory tracking performance of the two methods. The position tracking error for the developed method spikes at the start of the simulation, which can be accredited to the random initialization of the DNN weights.
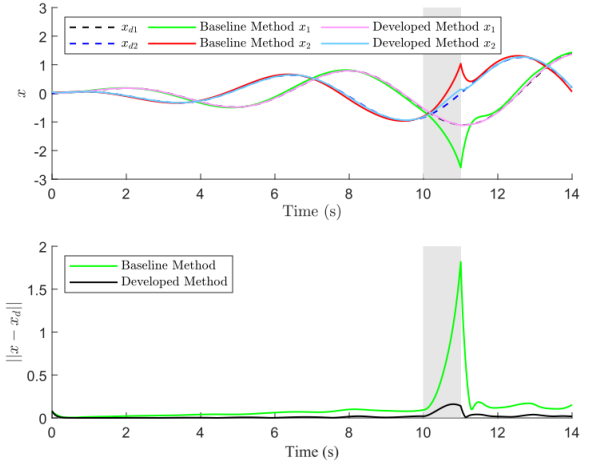

Figure 5. The top plot shows the desired versus actual value of each position state for the baseline and developed methods over the first 14 seconds of the simulation. The bottom plot shows the position tracking error for the two methods over the first 14 seconds of the simulation. The gray region represents the time period where state feedback is made unavailable.

The developed weight adaptation law in (13) helps to enable the position error to settle in less than 0.5 seconds. When feedback is lost at 10 seconds, the position error norm grows to a maximum value of 0.56 with the developed method compared to a value of 1.81 with the baseline method, thus achieving a 69.1% tracking performance improvement. The root mean square position error norm between 0 and 14 seconds is 0.035 with the developed method compared to 0.256 with the baseline method, thus achieving a 86.3% tracking performance improvement. The position tracking error from 14 seconds to 20 seconds is omitted from the plot because the desired trajectory in this timespan is outside of the safe set, rendering position error uninformative.

To demonstrate consistent safety performance across various reference trajectories and initial conditions, the sim-

Table I
PERFORMANCE RESULTS OVER 50 ITERATIONS

Control Method	Trajectory	Max. B	Avg. Max. B	Avg. Time Outside $\mathcal{S}$ (s)
Developed	Spiral 1	-0.18	-0.38	0
	Spiral 2	-0.13	-0.24	0
	Figure Eight	-0.05	-0.51	0
	Average	-0.12	-0.38	0
Baseline	Spiral 1	52.83	5.84	0.40
	Spiral 2	18.36	3.40	0.11
	Figure Eight	91.14	8.55	0.57
	Average	54.11	5.93	0.36

ulations were repeated for 50 iterations for three different desired trajectories. The three desired trajectories tested were the previously used spiral trajectory $x_d(t) = 0.1t[\sin(t),\ \cos(t)]^\top$ (henceforth referred to as "Spiral 1"), a second spiral trajectory defined as $x_d(t) = 0.075t[\sin(t),\ \cos(t)]^\top$ (henceforth referred to as "Spiral 2"), and a figure-eight trajectory defined as $x_d(t) = [2\sin(t),\ 2\sin(t)\cos(t)]^\top$. For each of the iterations for each of the three trajectories, the initial states were again randomly selected from the uniform distribution $U(-0.2, 0.2)$ with $\dot{x}(t_0) = [0,\ 0]^\top$, and the DNN weights were randomly initialized from the normal distribution $N(0, 0.5)$. The gains were kept the same as previously reported. Loss of feedback was simulated for two one-second periods, with the first instance of loss of feedback beginning at a time selected from the uniform distribution $U(0, 9)$ and the second instance of loss of feedback beginning at a time selected from the uniform distribution $U(10, 19)$. The performance results for each desired trajectory are shown in Table I. As can be seen in Table I, the maximum value of B for each trajectory across all iterations remains negative using the developed method. The negative value of B indicates that the developed aDCBF method successfully maintained the state inside the safe set at all times over each trajectory and each iteration, whereas, in the baseline method, the average time spent outside of the safe set over all three trajectories is 0.36 seconds, which is 18% of the time feedback was made unavailable. The developed aDCBF method yielded similar results across all iterations regardless of the desired trajectory used or differences in the initial DNN weights.

VII. CONCLUSION

This paper provides a method to ensure safety while learning the system's uncertain dynamics in real-time. The developed method is the first result that combines CBFs with an adaptive DNN that updates in real-time, eliminating the need for pre-training. Unlike previous Lb-DNN literature where the DNN adaptation laws are based on a tracking error, the developed DNN adaptation law is based on an identification error. The developed DNN adaptation law yields function approximation error convergence, which iss then used in an optimization-based control law that enforced forward invariance of the safe set. A combined Lyapunov-based analysis is proven to achieve guarantees on the DNN function approximation under the PE condition. Furthermore, to ensure

safety under intermittent loss of feedback, the developed aDCBF is extended by leveraging the learned DNN's capacity to extrapolate beyond the explored trajectory points. A switched systems analysis for CBFs is provided with a maximum dwell-time condition during which the feedback can be unavailable. Simulation results are provided for ACC and intermittent feedback system examples with comparisons to robust CBFs and observer-based CBFs as baselines. The developed aDCBF method ensured safety while reducing undesirable conservative behavior by 85.6%, compared to a robust CBF approach. Future work may involve extension to high-order aDCBFs that ensure safety for systems of higher relative degree.

REFERENCES

[1] A. D. Ames, X. Xu, J. W. Grizzle, and P. Tabuada, "Control barrier function based quadratic programs for safety critical systems," *IEEE Trans. Autom. Control*, vol. 62, no. 8, pp. 3861–3876, 2016.
[2] A. D. Ames, S. Coogan, M. Egerstedt, G. Notomista, K. Sreenath, and P. Tabuada, "Control barrier functions: Theory and applications," in *Proc. Eur. Control Conf.*, 2019, pp. 3420–3431.
[3] A. J. Taylor and A. D. Ames, "Adaptive safety with control barrier functions," in *Proc. Am. Control Conf.*, 2020, pp. 1399–1405.
[4] B. T. Lopez, J.-J. E. Slotine, and J. P. How, "Robust adaptive control barrier functions: An adaptive and data-driven approach to safety," *IEEE Control Syst. Lett.*, vol. 5, no. 3, pp. 1031–1036, 2020.
[5] M. H. Cohen and C. Belta, "High order robust adaptive control barrier functions and exponentially stabilizing adaptive control Lyapunov functions," in *Proc. Am. Control Conf.*, 2022.
[6] W. Xiao, C. A. Belta, and C. G. Cassandras, "Sufficient conditions for feasibility of optimal control problems using control barrier functions," *Automatica*, vol. 135, p. 109960, 2022.
[7] A. Isaly, O. Patil, R. G. Sanfelice, and W. E. Dixon, "Adaptive safety with multiple barrier functions using integral concurrent learning," in *Proc. Am. Control Conf.*, 2021, pp. 3719–3724.
[8] M. Srinivasan, A. Dabholkar, S. Coogan, and P. A. Vela, "Synthesis of control barrier functions using a supervised machine learning approach," in *Int. Conf. Intell. Robots and Syst.*, 2020, pp. 7139–7145.
[9] R. Cheng, G. Orosz, R. M. Murray, and J. W. Burdick, "End-to-end safe reinforcement learning through barrier functions for safety-critical continuous control tasks," in *Proc. AAAI Conf. Artif. Intell.*, vol. 33, 2019, pp. 3387–3395.
[10] A. Isaly, O. Patil, H. Sweatland, R. Sanfelice, and W. E. Dixon, "Adaptive safety with a RISE-based disturbance observer," *IEEE Trans. Autom. Control*, vol. 69, no. 7, pp. 4883–4890, 2024.
[11] D. R. Agrawal and D. Panagou, "Safe and robust observer-controller synthesis using control barrier functions," *IEEE Control Syst. Lett.*, vol. 7, pp. 127–132, 2010.
[12] A. Alan, T. G. Molnar, E. Das, A. D. Ames, and G. Orosz, "Disturbance observers for robust safety-critical control with control barrier functions," *IEEE Control Syst. Lett.*, vol. 7, pp. 1123–1128, 2023.
[13] J. Sun, J. Yang, and Z. Zeng, "Safety-critical control with control barrier function based on disturbance observer," *IEEE Trans. Autom. Control*, pp. 1–8, 2024.
[14] O. Patil, D. Le, M. Greene, and W. E. Dixon, "Lyapunov-derived control and adaptive update laws for inner and outer layer weights of a deep neural network," *IEEE Control Syst Lett.*, vol. 6, pp. 1855–1860, 2022.

[15] E. Vacchini, N. Sacchi, G. P. Incremona, and A. Ferrara, "Design of a deep neural network-based integral sliding mode control for nonlinear systems under fully unknown dynamics," *IEEE Control Syst. Lett.*, 2023.

[16] S. Li, H. T. Nguyen, and C. C. Cheah, "A theoretical framework for end-to-end learning of deep neural networks with applications to robotics," *IEEE Access*, vol. 11, pp. 21 992–22 006, 2023.

[17] O. S. Patil, E. J. Griffis, W. A. Makumi, and W. E. Dixon, "Composite adaptive Lyapunov-based deep neural network (Lb-DNN) controller," *arXiv preprint arXiv:1306.3432*, 2023.

[18] E. Griffis, O. Patil, W. Makumi, and W. E. Dixon, "Deep recurrent neural network-based observer for uncertain nonlinear systems," in *IFAC World Congr.*, 2023, pp. 6851–6856.

[19] O. S. Patil, D. M. Le, E. Griffis, and W. E. Dixon, "Deep residual neural network (ResNet)-based adaptive control: A Lyapunov-based approach," in *Proc. IEEE Conf. Decis. Control*, 2022, pp. 3487–3492.

[20] E. Griffis, O. Patil, Z. Bell, and W. E. Dixon, "Lyapunov-based long short-term memory (Lb-LSTM) neural network-based control," *IEEE Control Syst. Lett.*, vol. 7, pp. 2976–2981, 2023.

[21] D. S. Bernstein, *Matrix Mathematics*. Princeton university press, 2009.

[22] J. Chai and R. G. Sanfelice, "On notions and sufficient conditions for forward invariance of sets for hybrid dynamical systems," in *IEEE Conf. Decis. Control*, pp. 2869–2874.

[23] A. Isaly, M. Mamaghani, R. G. Sanfelice, and W. E. Dixon, "On the feasibility and continuity of feedback controllers defined by multiple control barrier functions," *IEEE Trans. Autom. Control*, vol. 69, no. 11, pp. 7326 – 7339, 2024.

[24] M. Maghenem and R. G. Sanfelice, "Sufficient conditions for forward invariance and contractivity in hybrid inclusions using barrier functions," *Automatica*, vol. 124, 2021.

[25] P. Kidger and T. Lyons, "Universal approximation with deep narrow networks," in *Conf. Learn. Theory*, 2020, pp. 2306–2327.

[26] F. L. Lewis, A. Yesildirek, and K. Liu, "Multilayer neural-net robot controller with guaranteed tracking performance," *IEEE Trans. on Neural Netw.*, vol. 7, no. 2, pp. 388–399, 1996.

[27] K. Kawaguchi, "Deep learning without poor local minima," *NeurIPS*, vol. 29, 2016.

[28] H. Lu and K. Kawaguchi, "Depth creates no bad local minima," *arXiv preprint arXiv:1702.08580*, 2017.

[29] S. Du, J. Lee, Y. Tian, A. Singh, and B. Poczos, "Gradient descent learns one-hidden-layer CNN: Dont be afraid of spurious local minima," in *Proc. 35th Int. Conf. Mach. Learn.*, vol. 80, Jul 2018, pp. 1339–1348.

[30] K. Kawaguchi and Y. Bengio, "Depth with nonlinearity creates no bad local minima in ResNets," *Neural Netw.*, vol. 118, pp. 167–174, 2019.

[31] I. Goodfellow, Y. Bengio, A. Courville, and Y. Bengio, *Deep Learning*. MIT press Cambridge, 2016, vol. 1.

[32] R. Hart, O. Patil, E. Griffis, and W. E. Dixon, "Deep Lyapunov-based physics-informed neural networks (DeLb-PINN) for adaptive control design," in *Proc. IEEE Conf. Decis. Control*, 2023, pp. 1511–1516.

[33] M. Krstic, I. Kanellakopoulos, and P. V. Kokotovic, *Nonlinear and Adaptive Control Design*. New York: John Wiley & Sons, 1995.

[34] J. J. Slotine and W. Li, "Composite adaptive control of robot manipulators," *Automatica*, vol. 25, no. 4, pp. 509–519, Jul. 1989.

[35] J. P. Aubin and H. Frankowska, *Set-valued analysis*. Birkhäuser, 2008.

[36] H.-Y. Chen, Z. Bell, P. Deptula, and W. E. Dixon, "A switched systems approach to path following with intermittent state feedback," *IEEE Trans. Robot.*, vol. 35, no. 3, pp. 725–733, 2019.

[37] A. Parikh, T.-H. Cheng, H.-Y. Chen, and W. E. Dixon, "A switched systems framework for guaranteed convergence of image-based observers with intermittent measurements," *IEEE Trans. Robot.*, vol. 33, no. 2, pp. 266–280, April 2017.

Omkar Sudhir Patil received his Bachelor of Technology (B.Tech.) degree in production and industrial engineering from Indian Institute of Technology (IIT) Delhi in 2018, where he was honored with the BOSS award for his outstanding bachelor's thesis project. In 2019, he joined the Nonlinear Controls and Robotics (NCR) Laboratory at the University of Florida under the guidance of Dr. Warren Dixon to pursue his doctoral studies. Omkar received his Master of Science (M.S.) degree in mechanical engineering in 2022 and Ph.D. in mechanical engineering in 2023 from the University of Florida. During his PhD studies, he was awarded the Graduate Student Research Award for outstanding research. In 2023, he started working as a postdoctoral research associate at NCR Laboratory, University of Florida. His research focuses on the development and application of innovative Lyapunov-based nonlinear, robust, and adaptive control techniques.

Warren E. Dixon received the Ph.D. degree in electrical engineering from Clemson University, Clemson, SC, USA, in 2000. He joined the Universidy of Florida, Gainesville, FL, USA, in 2004 and is now the Distinguished Professor, Dean's Leadership Professor, and Department Chair with the Department of Mechanical Aerospace Engineering. He was a Wigner Fellow and Research Staff Member with the Oak Ridge National Laboratory, Oak Ridge, TN, USA. His main research interest has been the development and application of Lyapunov-based control techniques for uncertain nonlinear systems. Dr. Dixon was the recipient of various early and mid-career awards and best paper awards. He is an ASME Fellow for contributions to adaptive control of uncertain nonlinear systems.
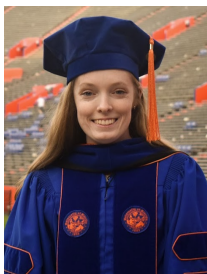
Hannah M. Sweatland received B.S, M.S., and Ph.D. degrees in mechanical engineering from the University of Florida, Gainesville, FL, USA in 2020, 2022, and 2024, respectively. Her research interests include safety of nonlinear systems, adaptive control, and passivity-based control.